galaxies

MDPI

Article

The Simplest Parametrization of the Equation of State Parameter in the Scalar Field Universe

Preeti Shrivastava [1,2], Abdul Junaid Khan [1], Mukesh Kumar [3], Gopikant Goswami [4], Jainendra Kumar Singh [5] and Anil Kumar Yadav [6,*]

1 Department of Mathematics, MATS University, Raipur 490006, India
2 Department of Mathematics, Shri Shankaracharya, Mahavidyalaya, Bhilai 490006, India
3 Department of Mathematics, GLA University, Mathura 281406, India
4 Department of Mathematics, Kalyan P. G. College, Bhilai 490006, India
5 Department of Mathematics, Netaji Subhas University of Technology, Delhi 110078, India
6 Department of Physics, United College of Engineering and Research, Greater Noida 201306, India
* Correspondence: abanilyadav@yahoo.co.in

Abstract: In this paper, we investigate a scalar field cosmological model of accelerating Universe with the simplest parametrization of the equation of state parameter of the scalar field. We use $H(z)$ data, pantheon compilation of SN Ia data and BAO data to constrain the model parameters using the χ^2 minimization technique. We obtain the present values of Hubble constant H_0 as $66.2^{+1.42}_{-1.34}$, $70.7^{+0.32}_{-0.31}$ and $67.74^{+1.24}_{-1.04}$ for $H(z)$, $H(z)$ + Pantheon and $H(z)$ + BAO respectively. In addition, we estimate the present age of the Universe in a derived model $t_0 = 14.38^{+0.63}_{-0.64}$ for joint $H(z)$ and pantheon compilation of SN Ia data which has only 0.88 σ tension with its empirical value obtained in Plank collaboration. Moreover, the present values of the deceleration parameter q_0 come out to be $-0.55^{+0.031}_{-0.038}$, $-0.61^{+0.030}_{-0.021}$ and $-0.627^{+0.022}_{-0.025}$ by bounding the Universe in the derived model with $H(z)$, $H(z)$ + Pantheon compilation of SN Ia and $H(z)$ + BAO data sets, respectively. We also have performed the state-finder diagnostics to discover the nature of dark energy.

Keywords: FRW Universe; scalar field model; parametrization of equation of state parameter

PACS: 98.80.-k; 04.20.Jb

Citation: Shrivastava, P.; Khan, A.J.; Kumar, M.; Goswami, G.; Singh, J.K.; Yadav, A.K. The Simplest Parametrization of the Equation of State Parameter in the Scalar Field Universe. *Galaxies* **2023**, *11*, 57. https://doi.org/10.3390/galaxies11020057

Academic Editors: Lorenzo Iorio and Orlando Luongo

Received: 24 January 2023
Revised: 28 March 2023
Accepted: 5 April 2023
Published: 17 April 2023

1. Introduction

We are living in a special epoch of cosmic history where the expansion of the Universe is not smooth or uniform, but it is speeding up which leads acceleration in the current Universe. However, the exact reason for this acceleration is still unknown. In the general theory of relativity, the late time acceleration of the Universe is described by inclusion of dark energy density along with matter density in Einstein's field equation [1–8], whereas in modified theories of gravity, some studies describe the current acceleration of the Universe without inclusion of a dark energy component [9–12]. The late time acceleration of the Universe has been investigated observationally using the luminosity distance of Supernovae type Ia (SN Ia) [13–16]. In addition to SN Ia observation, other observations, including baryon acoustic oscillation (BAO) [17], the cosmic microwave background (CMB) [18] and Plank collaboration [19] support an accelerated expansion of the Universe in the present epoch. The observational estimates suggest that the pressureless dark matter and hypothetical dark energy are two main ingredients of the Universe. However, the actual physics of these dark components of the Universe are still unknown. The simplest way to describe this acceleration of the Universe is that one has to assume a tiny cosmological constant Λ in Einstein field equations. The pressure of Λ is negative and equal to its energy density [20,21]. This type of cosmological model is known as the ΛCDM model, and it has received the greatest focus for its ability to fit most of the observational data. Despite

being consistent with observations, the ΛCDM model suffers from mainly two serious problems on theoretical grounds, namely the fine-tuning and the cosmic coincidence issue. Apart from these two issues, the ΛCDM model also suffers from H_0 tension which is one of the major problems at the present time within this paradigm. H_0 tension arises due to significant standard deviation in the estimated values of H_0 from the early measurements by the Planck team [22] and a model independent approach [23,24]. In Ref. [25], the authors elaborated on H_0 tension and its possible solution. Recently, Banerjee et al. [26] investigated that low redshift data comprising BAO, Cosmic Chronometers (CC) and SN Ia have a preference for quintessence models that lower H_0 relative to the ΛCDM model.

Another way to describe the late time acceleration of the Universe is to consider the Einstein–Hilbert Lagrangian as a generic function of the Ricci scalar R ($f(R)$ gravity) [27] or a function of the Ricci scalar R and the trace of energy momentum tensor T ($f(R,T)$ gravity) [9]. In 2014, Harko [28] studied the matter–geometry coupling of modified gravity models with thermodynamic implications. Some useful applications of the $f(R,T)$ theory of gravity are given in Refs. [12,29–34]. Furthermore, in Refs. [35,36], the authors constructed viable cosmological models in the $f(R)$ theory of gravity which qualify the solar system test. Some pioneer research in $f(R)$ gravity based on the galactic dynamic of massive test particles without inclusion of dark matter were investigated in Refs. [37–40]. Some other modified theories of gravity, such as $f(G)$ [41], $f(R,G)$ [42] and $f(T,B)$ [43] theories have been also investigated in recent times. A wide range of phenomena can be produced from modified theories of gravity by adopting different functions. However, many functional forms are not favored by recent cosmological observations. Recently, Nojiri et al. reviewed some standard issues and also the latest developments of modified theories of gravity [44]. In addition, we note that Oikonomou investigated a model of $f(R)$ gravity in the presence of a canonical scalar field which shows a unification of inflation with dark energy scenario [45]. Some useful applications of $f(R)$ gravity for describing the unifying of inflation with early and late dark energy epochs are given in Refs. [46–48]. Further, some applications of dark energy corrections are given in Refs. [49–51]. In particular, Yousaf [49] has investigated the stellar filaments with Minkowskian core in the Einstein - Λ gravity. In Ref. [50], the author has described the role of $f(G,T)$ terms in structure scalars. Furthermore, Yousaf et al. [51] have studied the causes of irregular energy density in f(R,T) gravity.

Apart from the modified theories of gravity or cosmological constant inspired models, the scalar fields with time or redshift varying equations of state are the most favored for producing acceleration in the Universe in the present epoch. The scalar field acquires negative pressure during slow roll down of scalar potential $V(\phi)$ [52–56]. The scalar field as a notion of tracker potentials in quintessence theory was introduced in Refs. [57–59]. These tracker-field-induced scalar field cosmological models avoid the fine-tuning and the coincidence problems. Johri [60] introduced the concept of integrated tracking which essentially shows that the tracker potentials follow a definite path of evolution of the Universe, in compatibility with the observational constraints. Some important applications of time varying equations of state parameters are discussed in Refs. [61–63]. In 2000, Sahni and Starobinsky [62] have given a clue that positive cosmological Lambda-term is a suitable candidate of dark energy. Later on, Sahni [61] has described the nature and dynamics of dark matter and dark energy. Chimento et al. [63] have investigated some scalar field cosmological models in Robertson-Walker space-time to describe the dynamics of the universe. The presence of a scalar field ϕ is also observed by several fundamental theories which motivate us to study the dynamic properties of scalar fields in cosmology. A wide range of scalar-field cosmological models was suggested so far [64–70]. Kamenshchik et al. [71] investigated a Chaplygin gas-type dark energy model with the peculiar equation of state parameter.

In this paper, we consider the parametrization of the equation of state parameter and obtain an explicit solution of Einstein field equations in flat FRW space time. The structure of this paper is as follows: In Section 2, the theoretical model and its basic equations are given. In Section 3, we present all the details of the observational data used in this paper

to constrain the cosmological parameters and their uncertainties. The physical properties of the Universe in the derived model are discussed in Section 4. Finally, in Section 5, we summarize our results focusing on the main ingredients of the model.

2. Theoretical Model and Basic Equations

We consider the following action for Einstein's field equations in the scalar field Universe.

$$S = S_g + S_m. \tag{1}$$

where S_g and S_m denote action due to gravitation and baryon matter, respectively.

The action due to gravitation is defined as

$$S_g = \int d^4x\sqrt{-g}\left[\frac{R}{16\pi G} + \left\{\frac{1}{2}g^{ij}\phi_i\phi_j - V(\phi)\right\}\right], \tag{2}$$

The action due to baryon matter is given by

$$S_m = \int \mathcal{L}\sqrt{-g}d^4x. \tag{3}$$

where $\mathcal{L}$ is the Lagrangian of baryon matter, and other symbols have their usual meaning.

Therefore, Einstein's field equation is recast as

$$R_{ij} - \frac{1}{2}Rg_{ij} = -8\pi G\, T_{ij} - \phi_i\phi_j + g_{ij}\left(\frac{1}{2}\phi^k\phi_k - V(\phi)\right). \tag{4}$$

In addition, the action S varies with respect to scalar field ϕ which leads to the following additional equation

$$\phi^i_{;i} + V'(\phi) = 0. \tag{5}$$

where $V'(\phi) = \frac{dV}{d\phi}$, and $V(\phi)$ denotes the scalar field potential.

The energy–momentum tensor for perfect fluid distribution is read as

$$T^{ij}_m = (p+\rho)u^iu^j - pg^{ij}. \tag{6}$$

where $g_{ij}u^iu^j = 1$.

The FLRW space–time (in unit $c = 1$) is given by

$$ds^2 = dt^2 - a(t)^2\left[dx^2 + dy^2 + dz^2\right]. \tag{7}$$

where $a(t)$ is the scale factor which defines the rate of expansion along the spatial direction.

In co-moving coordinates, $u^i = 0;\ i = 1, 2\ or\ 3$.

Since the space–time (7) spatially represents a homogeneous and isotropic Universe, one can consider a time varying scalar field, i.e., $\phi = \phi(t)$.

The field Equations (4) and (5) for metric (7) are read as

$$2\frac{\ddot{a}}{a} + H^2 = -8\pi G\left(\frac{\dot{\phi}^2}{2} - V(\phi)\right), \tag{8}$$

$$3H^2 = 8\pi G\left(\rho_m + \frac{\dot{\phi}^2}{2} + V(\phi)\right),\ H = \frac{\dot{a}}{a}. \tag{9}$$

and

$$\ddot{\phi} + 3H\dot{\phi} + V'(\phi) = 0. \tag{10}$$

Equation (10) is recast as

$$\frac{d}{dt}\left[\frac{1}{2}\dot{\phi}^2 + V(\phi)\right] + 3\frac{\dot{a}}{a}\dot{\phi}^2 = 0. \tag{11}$$

Thus, the energy momentum tensor of the scalar field is obtained as

$$T_{\phi}^{ij} = (p_{\phi} + \rho_{\phi})u^i u^j - p_{\phi} g^{ij}. \tag{12}$$

where $\rho_{\phi} = \frac{1}{2}\dot{\phi}^2 + V(\phi)$, and $p_{\phi} = \frac{1}{2}\dot{\phi}^2 - V(\phi)$.

Now, the equation of state parameter for the scalar field is defined as $\omega_{\phi} = \frac{p_{\phi}}{\rho_{\phi}}$.

Hence, the scalar field potential in terms of ω_{ϕ} is computed as

$$V(\phi) = \frac{1 - \omega_{\phi}}{2(1 + \omega_{\phi})}\dot{\phi}^2. \tag{13}$$

From Equations (8)–(10), we observe that there are three equations with four H, ρ_m, ϕ and V variables. Hence, one cannot solve these equations in general. However, to obtain an explicit solution to the above equations, we have to assume at least one reasonable relationship among the variables or parameterize the variables. That is why we have considered the simplest parametrization of the equation of state parameter of the scalar field, given by Gong and Zhang [72]

$$\omega_{\phi} = \frac{(\omega_{\phi})_0}{1 + z}. \tag{14}$$

where $(\omega_{\phi})_0$ denotes the present value of the equation of state parameter of the scalar field. The main reason for considering parametrization of ω_{ϕ} in the form of Equation (14) is that at $z = 0$ it gives $\omega_{\phi} = (\omega_{\phi})_0$ and as $z \to \infty$, $\omega_{\phi} \to 0$ which is eventually true for modeling the observed Universe. The parametrization of the equation of state parameter of the scalar field given in Equation (14) is not unique ,and it has been implemented in several studies. It is worth noting that our method of finding a solution and procedure of performing data fitting are altogether different.

Using Equations (13) and (14), Equation (11) reduces to

$$\frac{d}{dt}\left[\frac{1}{2}\dot{\phi}^2 + \frac{1 + z - (\omega_{\phi})_0}{2[1 + z + (\omega_{\phi})_0]}\dot{\phi}^2\right] + 3\frac{\dot{a}}{a}\dot{\phi}^2 = 0. \tag{15}$$

Integrating Equation (15), we obtain

$$\dot{\phi}^2 = \dot{\phi}_0^2 \frac{(\omega_{\phi})_0 + z + 1}{(\omega_{\phi})_0 + 1}(z + 1)^2 \, exp\left[\frac{3(\omega_{\phi})_0 z}{z + 1}\right]. \tag{16}$$

where $\dot{\phi}_0$ denotes the value of $\dot{\phi}$ at $z = 0$.

Thus, the expression for ρ_{ϕ} and p_{ϕ} are read as

$$\rho_{\phi} = \frac{1}{2}\dot{\phi}^2 + V(\phi) = (\rho_{\phi})_0(z + 1)^3 exp\left[\frac{3(\omega_{\phi})_0 z}{z+1}\right]. \tag{17}$$

$$p_{\phi} = \omega_{\phi}\rho_{\phi} = \frac{(\omega_{\phi})_0}{1 + z}\rho_{\phi}. \tag{18}$$

The continuity equation is given as

$$\dot{\rho_m} + 3\rho_m H + \dot{\rho_{\phi}} + 3(\rho_{\phi} + p_{\phi})H = 0. \tag{19}$$

From Equation (19), one may argue that the baryon matter component and the scalar field component are conserved separately. For the scalar field component, $\dot{\rho_\phi} + 3(\rho_\phi + p_\phi)H = 0$ which will be easily obtained from Equation (10) or Equation (11) by solving $\rho_\phi = \frac{1}{2}\dot{\phi}^2 + V(\phi)$ and $p_\phi = \frac{1}{2}\dot{\phi}^2 - V(\phi)$. Therefore, Equations (11) and (19) lead to

$$\dot{\rho_m} + 3\rho_m H = 0. \tag{20}$$

Integrating Equation (20), we obtain

$$\rho_m = (\rho_m)_0(1+z)^3. \tag{21}$$

Here, the parameters with suffix 0 denote its present value.

From Equations (8) and (9), the expression for deceleration parameter q and Hubble's parameter H are, respectively, obtained as

$$2q = 1 + \frac{3(\omega_\phi)_0(\Omega_\phi)_0\, exp\left(\frac{3(\omega_\phi)_0 z}{z+1}\right)}{(1+z)\left[(1-\Omega_\phi)_0 + (\Omega_\phi)_0\, exp\left(\frac{3(\omega_\phi)_0 z}{z+1}\right)\right]}. \tag{22}$$

$$H(z) = H_0\sqrt{(1+z)^3\left[(1-\Omega_\phi)_0 + (\Omega_\phi)_0\, exp\left(\frac{3(\omega_\phi)_0 z}{z+1}\right)\right]}. \tag{23}$$

The luminosity distance is read as

$$D_L = (1+z)\int_0^z \frac{dz}{H(z)}. \tag{24}$$

Thus, the distance modulus μ is obtained as

$$\mu = m - M = 5log_{10}D_L(z) + \mu_0. \tag{25}$$

where m and M are apparent magnitude and absolute magnitude of any distant luminous object, respectively. $\mu_0 = 5log_{10}\left(H_0^{-1}/Mpc\right) + 25$ is the marginalized nuisance parameter.

3. Observational Constraints

In this section, we use 46 $H(z)$ data sets, Pantheon compilation of SN Ia data and Baryon Acoustic Oscillation (BAO) data sets to constrain the model parameters of the Universe in the derived model. Note that the complete list of $H(z)$ data points are compiled in Refs. [73,74] and Appendix A of this paper. The pantheon compilation of SN Ia data in the redshift range $0.01 < z < 2.3$ is given in Scolnic et al. [75]. ,We consider the third data set to be the Baryon Acoustic Oscillation (BAO) data which includes six distinct measurements of the baryon acoustic scale. The BAO data points are summarized in Table 1.

Table 1. The BAO data points which we use in our analysis.

S. N.	z	d_i	References
1	0.106	0.336	[76]
2	0.35	0.113	[77]
3	0.57	0.073	[78]
4	0.44	0.0916	[79]
5	0.60	0.0726	[79]
6	0.73	0.0592	[17]

To obtain χ^2_{BAO}, we adopt the same procedure as given in Ref. [80]. Therefore, χ^2_{BAO} is computed as

$$\chi^2_{BAO} = X^T C^{-1}_{BAO} X, \tag{26}$$

where $X = [d(0.106) - 0.336, \frac{1}{d(0.35)} - \frac{1}{0.113}, \frac{1}{d(0.57)} - \frac{1}{0.073}, d(0.44) - 0.0916, d(0.6) - 0.0726, d(0.73) - 0.0592]$, and $d(z) = \frac{r_s(z_{drag})}{D_V(z)}$, with $r_s(a) = \int_0^a \frac{c_s da}{a^2 H(a)}$, is the co-moving sound horizon at the baryon drag epoch, c_s the baryon sound speed and $D_V(z)$ is defined as $D_V(z) = \left[(1+z)^2 D_A^2(z) \frac{z}{H(z)}\right]^{\frac{1}{3}}$. Here, $D_A(z)$ is the angular diameter distance.

The χ^2 for $H(z)$ data is read as

$$\chi^2_{H(z)} = \sum_{i=1} \left[\frac{H_{th}(z_i) - H_{obs}(z_i)}{\sigma_i}\right]^2, \tag{27}$$

where $H_{th}(z_i)$ and $H_{obs}(z_i)$ denote the theoretical and observed values, respectively, and σ_i^2 denotes the standard deviation of each $H_{obs}(z_i)$.

Since these data sets are independent from one another, the joint χ^2 is obtained as

$$\chi^2_{H(z)+Pantheon} = \chi^2_{H(z)} + \chi^2_{Pantheon}. \tag{28}$$

and

$$\chi^2_{H(z)+BAO} = \chi^2_{H(z)} + \chi^2_{BAO}. \tag{29}$$

Figures 1–6 depict two-dimensional contours at 1σ, 2σ and 3σ confidence regions by bounding our model with $H(z)$, $H(z)$ + pantheon compilation of Sn Ia data and $H(z)$ + BAO data, respectively. The result of this analysis is summarized in Table 2.

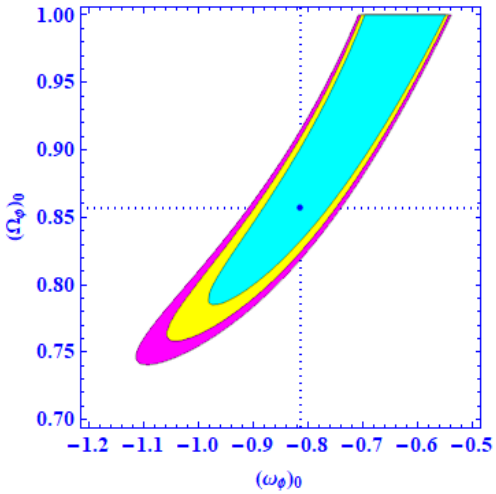

Figure 1. Two-dimensional contours in the $(\omega_\phi)_0 - (\Omega_\phi)_0$ plane at 1σ, 2σ and 3σ confidence regions by bounding our model with $H(z)$ data.

Table 2. Constrained values of model parameters.

Parameters	$H(z)$	$H(z)$ + Pantheon	$H(z)$ + BAO
H_0	$66.2^{+1.42}_{-1.34}$	$70.13^{+0.42}_{-0.41}$	$67.74^{+1.24}_{-1.04}$
$(\Omega_\phi)_0$	$0.857^{+0.041}_{-0.025}$	$0.856^{+0.031}_{-0.020}$	$0.885^{+0.048}_{-0.046}$
$(\omega_\phi)_0$	$-0.815^{+0.066}_{-0.050}$	$-0.869^{+0.046}_{-0.045}$	$-0.849^{+0.028}_{-0.027}$

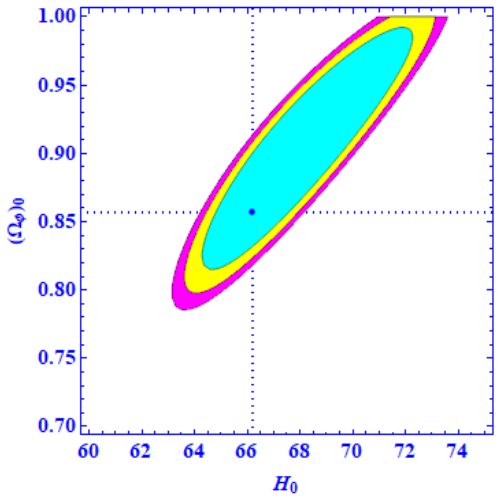

Figure 2. Two-dimensional contours in the $H_0 - (\Omega_\phi)_0$ plane at 1σ, 2σ and 3σ confidence regions by bounding our model with $H(z)$ data

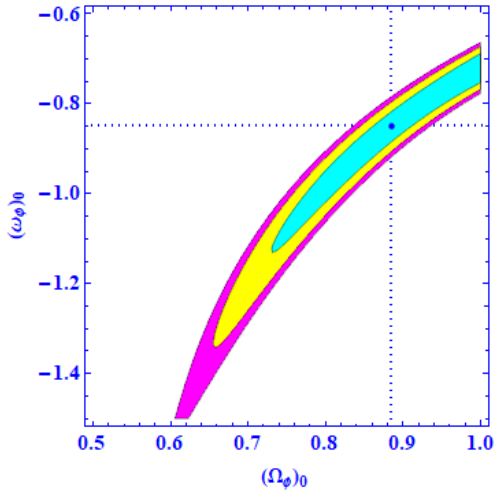

Figure 3. Two-dimensional contours in the $(\Omega_\phi)_0 - (\omega_\phi)_0$ plane at 1σ, 2σ and 3σ confidence regions by bounding our model with joint $H(z)$ and pantheon compilation of SN Ia data.

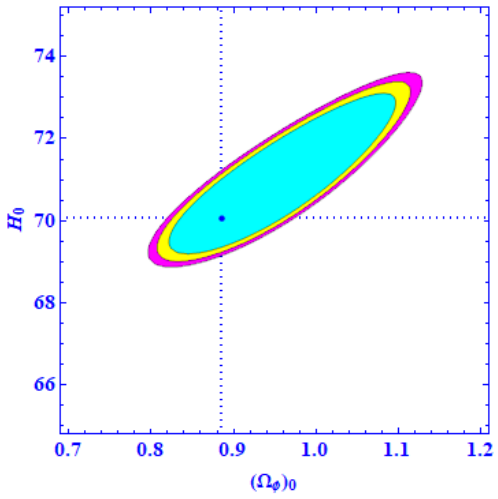

Figure 4. Two-dimensional contours in the $(\Omega_\phi)_0 - H_0$ plane at 1σ, 2σ and 3σ confidence regions by bounding our model with joint $H(z)$ and pantheon compilation of SN Ia data.

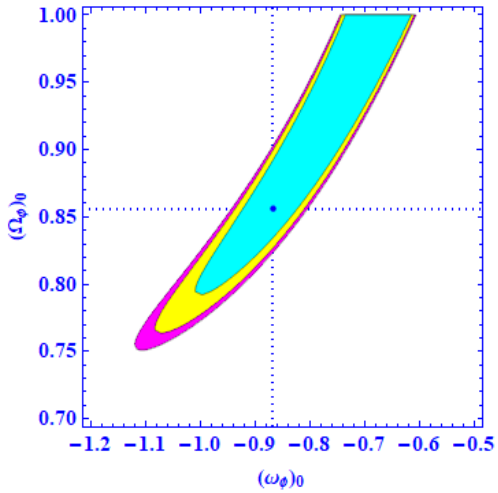

Figure 5. Two-dimensional contours in the $(\omega_\phi)_0 - (\Omega_\phi)_0$ plane at 1σ, 2σ and 3σ confidence regions by bounding our model with joint $H(z)$ and BAO data.

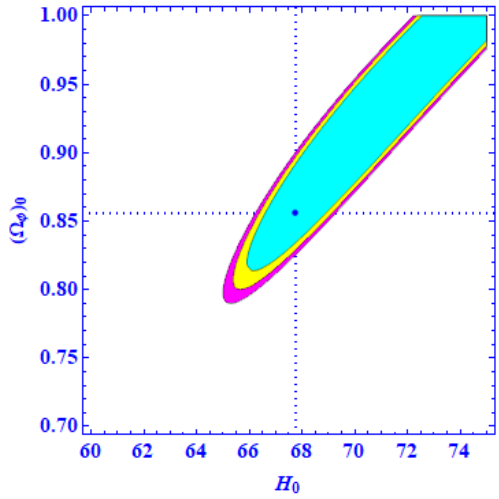

Figure 6. Two-dimensional contours in the $(H_0 - (\Omega_\phi)_0$ plane at 1σ, 2σ and 3σ confidence regions by bounding our model with joint $H(z)$ and BAO data.

4. Physical Properties of The Model

4.1. Age of Universe

The age of the Universe in the derived model is computed as

$$H_0(t_0 - t) = \int_0^z \frac{dz}{(1+z)h(z)}; \; h(z) = H(z)/H_0. \tag{30}$$

Therefore, the present age of the Universe is obtained as

$$H_0 t_0 = \lim_{z\to\infty} \int_0^z \frac{dz}{(1+z)h(z)}. \tag{31}$$

where t_0 denotes the present age of the Universe.

Figure 7 depicts the variation of $H_0(t_0 - t)$ with respect to redshift z. Note that we considered the estimated values of H_0, $(\Omega_\phi)_0$ and $(\omega_\phi)_0$ in this paper by bounding the derived model with $H(z)$, $H(z)$ + Pantheon and $H(z)$ + BAO data sets. Integrating Equation (31) for the values of H_0, $(\Omega_\phi)_0$ and $(\omega_\phi)_0$ given in Table 2, we obtain the present age of the Universe t_0 in this paper for $H(z)$, $H(z)$ + Pantheon compilation of SN Ia data and $H(z)$ + BAO data sets as $14.45^{+0.316}_{-0.311}$ Gyrs, $14.38^{+0.63}_{-0.64}$ Gyrs and $14.42^{+0.22}_{-0.25}$ Gyrs, respectively. It is worth noting that the empirical age of the Universe extracted in a Plank collaboration result [19]

is given as $t_0 = 13.81^{+0.038}_{-0.038}$ Gyrs. In some other cosmological studies, the present age of the Universe is computed as $14.46^{+0.8}_{-0.8}$ Gyrs [81], $14.3^{+0.6}_{-0.6}$ Gyrs [82], $14.61^{+0.22}_{-0.22}$ Gyrs [83] and $14.5^{+1.5}_{-1.5}$ Gyrs [84]. Thus, we observe that the age of the Universe estimated in the derived model is in good agreement with its value extracted in Plank collaboration [19]. It is important to note that the estimated age of the Universe due to joint $H(z)$ and Pantheon compilation of SN Ia data in this paper, i.e., $t_0 = 14.38^{+0.63}_{-0.64}$ has only 0.88 σ tension with the Plank collaboration result [19]. Some useful remarks on the age of the Universe and its curvature are given in Ref. [85].

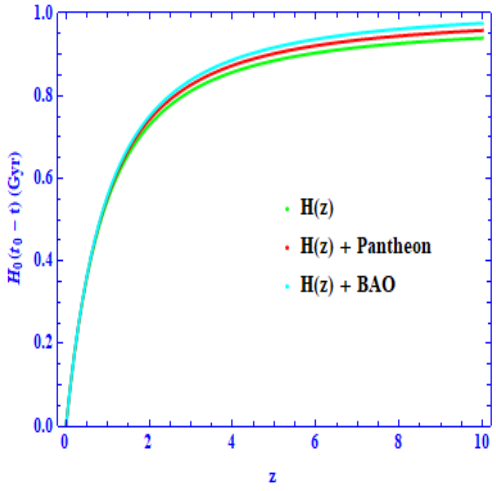

Figure 7. Plot of $H_0(t_0 - t)$ versus redshift z.

4.2. Deceleration Parameter

Equation (22) is recast as

$$q = \frac{1}{2}\left[1 + \frac{3(\omega_\phi)_0(\Omega_\phi)_0\, exp\left(\frac{3(\omega_\phi)_0 z}{z+1}\right)}{(1+z)\left[(\Omega_m)_0 + (\Omega_\phi)_0\, exp\left(\frac{3(\omega_\phi)_0 z}{z+1}\right)\right]}\right]. \tag{32}$$

Figure 8 depicts the dynamics of deceleration parameter q with respect to redshift z for $H(z)$ data (left panel, $H(z)$ + Pantheon compilation of SN Ia data (middle panel) and $H(z)$ + BAO data (right panel). We obtain the present value of deceleration parameter q_0 as $-0.55^{+0.031}_{-0.038}$, $-0.61^{+0.030}_{-0.021}$ and $-0.627^{+0.022}_{-0.025}$ by bounding the Universe in the derived model with $H(z)$, $H(z)$ + Pantheon compilation of SN Ia and $H(z)$ + BAO data sets, respectively. Figure 9 shows a single plot of q versus z. Recently, Capozziello et al. [86] obtained the empirical value of q_0 as $-0.56^{+0.04}_{-0.04}$. Some other empirical values of q_0 in the vicinity of our obtained values of q_0 are given in Refs. [87–92].

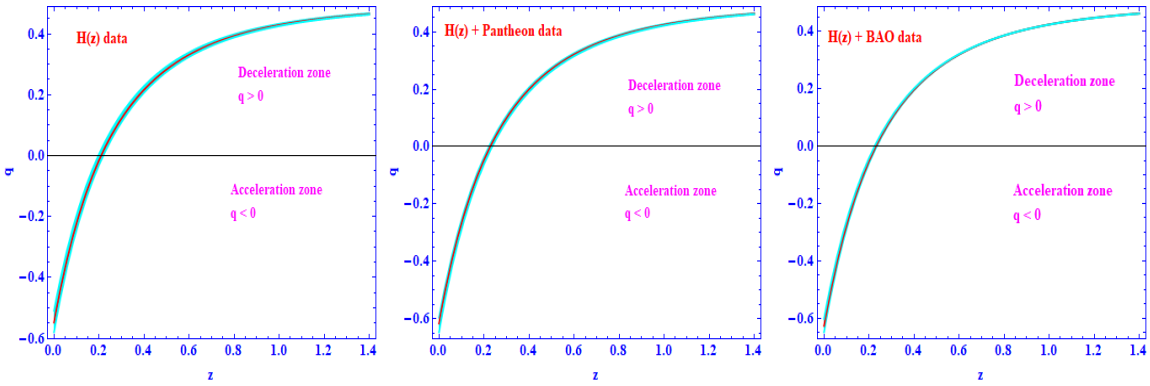

Figure 8. Variation of deceleration parameter versus redshift z for $H(z)$ data (left panel, $H(z)$ + Pantheon compilation of SN Ia data (middle panel) and $H(z)$ + BAO data (right panel).

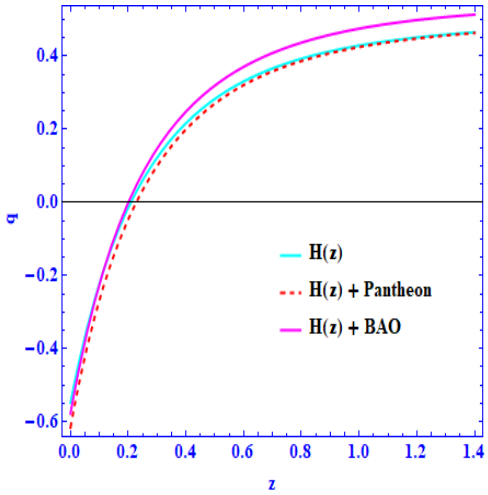

Figure 9. Single plot of q versus redshift z.

4.3. Statefinder Diagnostics

The statefinder pairs $\{r, s\}$ are the geometrical quantities which are directly obtained from the metric. This diagnostic is used to distinguish different dark energy models and hence becomes an important tool in modern cosmology. Alam et al. [93,94] defined the statefinder parameters r and s as follows

$$r = \frac{\dddot{a}}{aH^3} \quad , \quad s = \frac{r-1}{3(q-\frac{1}{2})}. \tag{33}$$

Figures 10 and 11 exhibit the behaviour of r and s with respect to z, respectively. We compute $r = 0.4.54$ and $s = -1.05$ for joint $H(z)$ and pantheon compilation of SN Ia data at $z = 0$. From Figures 10 and 11, we observe that $r > 1$ and $s < 0$ in the redshift range $\{0, 20\}$. In addition, the Universe in the derived model presumes the values of statefinder pairs in the range $r > 1$ and $s < 0$ and therefore represents a Chaplygin gas-type dark energy model (CGDE). We draw the temporal evolution of the Universe mimicked by our model in Figure 12. The trajectory in the $r - s$ plane clearly shows that the profile starts from the region $r > 1$ and $s < 0$ which corresponds to the CGDE Universe.

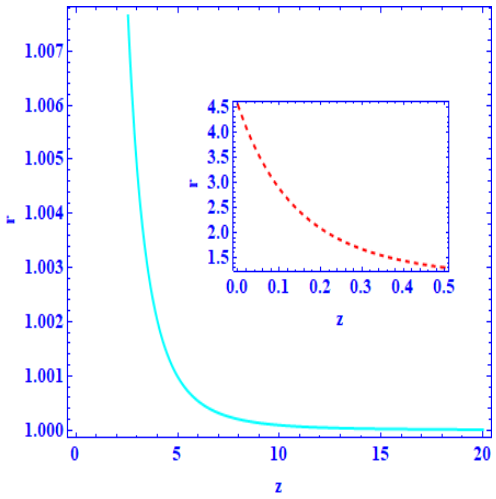

Figure 10. Plot of r versus z.

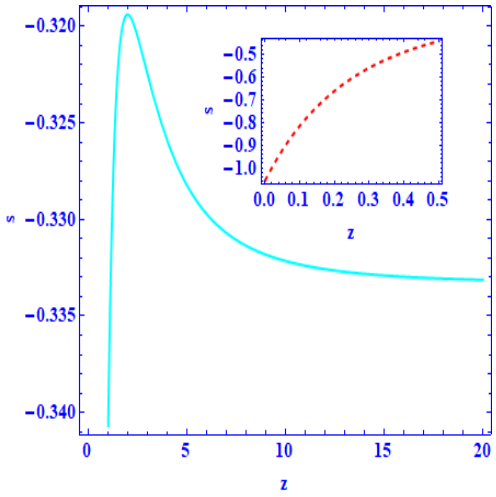

Figure 11. Plot of s versus z.

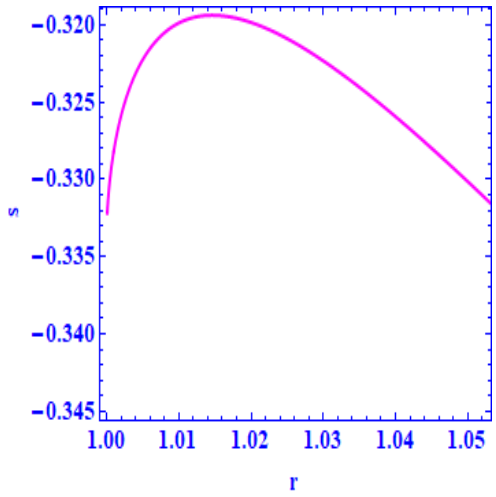

Figure 12. Trajectory in the $r - s$ plane.

The expression of r in terms of q and z is obtained as

$$r = (2q + 1)q + (1 + z)\frac{dq}{dz}. \tag{34}$$

5. Concluding Remarks

In this paper, we have investigated the late time accelerated expansion of the Universe by taking into account the scalar field with positive potential. To obtain an explicit solution of the field equations, we considered the simplest parametrization of the equation of state parameter $\omega_\phi = \frac{(\omega)_0}{1+z}$. This parametrization gives $\omega_\phi = (\omega)_0$ at the present epoch. The scalar field potential $V(\phi)$ is directly connected to pressure through equation $p_\phi = \frac{1}{2}\dot{\phi}^2 - V(\phi)$; therefore, the pressure p_ϕ is negative when $V(\phi) > \frac{1}{2}\dot{\phi}^2$, and hence, $V(\phi)$ is responsible for negative pressure that leads the acceleration of the Universe in the derived model. We used $H(z)$ data, Pantheon compilation of SN Ia data and BAO data to constrain the model parameters using a χ^2 minimization technique. The constrained values of H_0, $(\Omega_\phi)_0$ and $(\omega_\phi)_0$ from all data sets are given in Table 2.

Furthermore, we also estimated the present age of the Universe as $14.45^{+0.316}_{-0.311}$ Gyrs, $14.38^{+0.63}_{-0.64}$ Gyrs and $14.42^{+0.22}_{-0.25}$ Gyrs by using $H(z)$, $H(z)$ + Pantheon compilation of SN Ia data and $H(z)$ + BAO data, respectively. Moreover, our estimated age of the Universe in the derived model due to combined $H(z)$ and Pantheon compilation of SN Ia data has only 0.88 σ tension compared to the Plank collaboration results [19]. In additon, the values of H_0 tensions that we obtain are 0.37 σ and 6.5 σ for combined $H(z)$ and BAO data and combined H(z) and Pantheon compilation of SN Ia data, respectively, when we compare our results with the value of H_0 given in Plank collaboration [22]. Moreover, the H_0 tensions in this paper are 3.3 σ and 2.62 σ for combined $H(z)$ and BAO data and combined H(z) and Pantheon compilation of SN Ia data, respectively, in comparing our H_0 value with R19 [23]. The Universe in the derived model evolves with a positive deceleration parameter in its early phase of expansion, and after dominance of the scalar field, the Universe evolves with a negative value of the deceleration parameter which shows a transition from an early decelerated expanding phase to the current accelerated expanding phase. It is interesting to note the value of $q_0 = -0.55^{+0.031}_{-0.038}$ obtained in our model is in good agreement with the recent results as reported in Ref. [86]. Furthermore, to investigate the parametrization from a geometrical point of view, we also diagnose the statefinder pairs $\{r, s\}$. We observe that the Universe in the derived model describes a Chaplygin gas-type dark energy model (CGDE). Furthermore, we note that the authors of Refs. [95,96] use similar data sets for constraining the observational parameters of the Universe. In Bouali et al. [96], the present acceleration of the Universe is described by taking into consideration the parameterized deceleration parameter $q(z)$. As a final comment, we note from the above comparative study that the present model may be a viable model to describe the late time acceleration of the Universe and observational constraint update for the scalar field as dark energy.

Author Contributions: P.S.: Writing—original draft. A.J.K.: Review & editing. M.K.: Writing—original draft, Methodology, Writing—review & editing. G.G.: Writing—original draft, Writing—review & editing. J.K.S.: Review & editing. A.K.Y.: Writing—original draft, Conceptualization, Methodology, Writing—review & editing. All authors have read and agreed to the published version of the manuscript.

Funding: This research received no external funding.

Data Availability Statement: The data underlying this article will be shared on reasonable request to the authors.

Acknowledgments: The authors wish to place on record their sincere thanks to the reviewer(s) for illuminating suggestions that have significantly improved our manuscript in terms of research quality.

Conflicts of Interest: The authors declare no conflict of interest.

Appendix A

Table A1. Hubble parameter H(z) with redshift and errors σ_i.

S. N.	z	H(z)	σ_i	Method	References
1	0	67.77	1.30	DA	[97]
2	0.07	69	19.6	DA	[98]
3	0.09	69	12	DA	[99]
4	0.01	69	12	DA	[100]
5	0.12	68.6	26.2	DA	[98]
6	0.17	83	8	DA	[100]
7	0.179	75	4	DA	[101]
8	0.1993	75	5	DA	[101]
9	0.2	72.9	29.6	DA	[98]
10	0.24	79.7	2.7	DA	[102]
11	0.27	77	14	DA	[100]
12	0.28	88.8	36.6	DA	[98]
13	0.35	82.7	8.4	DA	[103]
14	0.352	83	14	DA	[101]
15	0.38	81.5	1.9	DA	[104]
16	0.3802	83	13.5	DA	[105]
17	0.4	95	17	DA	[99]
18	0.4004	77	10.2	DA	[105]
19	0.4247	87.1	11.2	DA	[105]
20	0.43	86.5	3.7	DA	[102]
21	0.44	82.6	7.8	DA	[106]
22	0.44497	92.8	12.9	DA	[105]
23	0.47	89	49.6	DA	[107]
24	0.4783	80.9	9	DA	[105]
25	0.48	97	60	DA	[100]
26	0.51	90.4	1.9	DA	[104]
27	0.57	96.8	3.4	DA	[108]
28	0.593	104	13	DA	[101]
29	0.6	87.9	6.1	DA	[106]
30	0.61	97.3	2.1	DA	[104]
31	0.68	92	8	DA	[101]
32	0.73	97.3	7	DA	[106]
33	0.781	105	12	DA	[101]
34	0.875	125	17	DA	[101]
35	0.88	90	40	DA	[100]
36	0.9	117	23	DA	[100]
37	1.037	154	20	DA	[101]
38	1.3	168	17	DA	[100]
39	1.363	160	33.6	DA	[109]
40	1.43	177	18	DA	[100]
41	1.53	140	14	DA	[100]
42	1.75	202	40	DA	[100]
43	1.965	186.5	50.4	DA	[109]
44	2.3	224	8	DA	[110]
45	2.34	222	7	DA	[111]
46	2.36	226	8	DA	[112]

References

1. Kumar, S.; Yadav, A.K. Some Bianchi type V models of accelerating universe with dark energy. *Mod. Phys. Lett. A* **2011**, *26*, 647. [CrossRef]
2. Yadav, A.K. Some anisotropic dark energy models in Bianchi type-V space-time. *Astrophys. Space Sc.* **2011**, *335*, 565. [CrossRef]
3. Yadav, A.K. A transitioning universe with anisotropic dark energy. *Astrophys. Space Sc.* **2016**, *361*, 1. [CrossRef]
4. Goswami, G.K.; Yadav, A.K.; Mishra, B. Probing kinematics and fate of Bianchi type V Universe. *Mod. Phys. Lett. A* **2020**, *35*, 2050224. [CrossRef]
5. Amirhashchi, H.; Yadav, A.K.; Ahmad, N.; Yadav, V. Interacting Dark Sectors in Anisotropic Universe: Observational Constraints and H_0 Tension. *Phys. Dark Uni.* **2022**, *36*, 2022. [CrossRef]

6. Goswami, G.K.; Mishra, M.; Yadav, A.K.; Pradhan, A. Two Fluid Scenario in Bianchi Type-I Universe. *Mod. Phys. Lett. A* **2020**, *33*, 2050086. [CrossRef]
7. Kumar, S.; Singh, C.P. Anisotropic dark energy models with constant deceleration parameter. *Gen. Relativ. Grav.* **2011**, *43*, 1427. [CrossRef]
8. Akarsu, Ö; Kılınc, C.B. Bianchi type III models with anisotropic dark energy. *Gen. Relativ. Grav.* **2010**, *42*, 763. [CrossRef]
9. Harko, T.; Lobo, F.S.N.; Nojiri, S.; Odintsov, S.D. $f(R,T)$ gravity. *Phys. Rev. D* **2011**, **84**, 024020. [CrossRef]
10. Prasad, R.; Gupta, L.K.; Goswami, G.K.; Yadav, A.K. Bulk viscous accelerating Universe in $f(R,T)$ theory of gravity. *Pramana J. Physics* **2020**, *94*, 135. [CrossRef]
11. Yadav, A.K.; Sahoo, P.K.; Bhardwaj, V. Bulk Viscous Bianchi-I Embedded Cosmological Model in $f(R,T) = f_1(R) + f_2(R)f_3(T)$ Gravity. *Mod. Phys. Lett. A* **2019**, *34*, 1950145. [CrossRef]
12. Sharma, L.K.; Yadav, A.K.; Sahoo, P.K.; Singh, B.K. Non-Minimal Matter-Geometry Coupling in Bianchi-I Space-Time. *Results Phys.* **2018**, *10*, 738. [CrossRef]
13. Perlmutter, S.; Gabi, S.; Goldhaber, G.; Goobar, A.; Groom, D.E.; Hook, I.M.; Kim, A.G.; Kim, M.Y. ; Lee, J.C.; Pain, R.; et al. Measurements of the Cosmological Parameters Ω and Λ from the First Seven Supernovae at $z \geq 0.35$. *ApJ* **1997**, *483*, 565. [CrossRef]
14. Perlmutter, S.; Aldering, G.; Della Valle, M.; Deustua, S.; Ellis, R.S.; Fabbro, S.; Fruchter, A.; Goldhaber, G.; Groom, D.E.; Hook, I.M.; et al. Discovery of a supernova explosion at half the age of the Universe. *Nature* **1998**, *391*, 51. [CrossRef]
15. Perlmutter, S.; Aldering, G.; Goldhaber, G.; Knop, R.A.; Nugent, P.; Castro, P.G. ; Deustua, S.; Fabbro, S.; Goobar, A.; Groom, D.E.; Hook, I.M.; et al. Measurements of Ω and Λ from 42 High-Redshift Supernovae. *ApJ* **1999**, *517*, 565. [CrossRef]
16. Riess, A.G.; Strolger, L.-G.; Tonry, J.; Casertano, S.; Ferguson, H.C.; Mobasher, B.; Challis, P.; Filippenko, A.V.; Jha, S.; Li, W.; et al. Type Ia supernova discoveries at $z > 1$ from the Hubble space telescope: Evidence for past deceleration and constraints on dark energy evolution. *ApJ* **2004**, *607*, 665. [CrossRef]
17. Blake, C.; Kazin, E.; Beutler, F.; Davis, T.; Parkinson D.; Brough, S.; Colless, M.; Contreras, C.; Couch, W.; Croom, S.; et al. The WiggleZ Dark Energy Survey: Mapping the distance-redshift relation with baryon acoustic oscillations. *MNRAS* **2011**, *418*, 1707. [CrossRef]
18. Bennett, C.; Hill, R. S.; Hinshaw, G.; Nolta, M. R.; Odegard, N.; Page, L.; Spergel, D. N.; Weiland, J. L.; Wright, E. L.; Halpern, M.; et al. First-Year Wilkinson Microwave Anisotropy Probe (WMAP) Observations: Foreground Emission. *ApJS* **2003**, *148*, 1. [CrossRef]
19. Ade, P.A.R.; Aghanim, N.; Arnaud, M.; Ashdown, M.; Aumont, J.; Baccigalupi, C.; Banday, A.J.; Barreiro, R.B.; Bartlett, J.G.; Bartolo, N.; et al. [Planck Collaboration.] Planck 2015 results XIII Cosmological parameters. *Astron. Astrophys.* **2016**, *594*, A13.
20. Weinberg, S. The cosmological constant problem. *Rev. Mod. Phys.* **1989**, *61*, 1. [CrossRef]
21. Peebles, P.; Ratra, B. The cosmological constant and dark energy. *Rev. Mod. Phys.* **2003**, *75*, 559. [CrossRef]
22. Aghanim, N.; Akrami Y.; Ashdown, M.; Aumont, J.; Baccigalupi, C.; Ballardini, M.; Banday, A.J.; Barreiro, R.B.; Bartolo, N.; Basak, S.; et al. Planck 2018 results. VI. Cosmological parameters. *arXiv* **2018**, arXiv:1807.06209.
23. Riess, A.G.; Casertano, S.; Yuan, W.; Macri, L.M.; Scolnic, D. Large magellanic cloud cepheid standards provide a 1% foundation for the determination of the Hubble Constant and stronger evidence for Physics beyond ΛCDM. *Astrophys. J.* **2019**, *876*, 85. [CrossRef]
24. Riess, A.G.; Casertano, S.; Yuan, W.; Bowers, J.B.; Macri, L.; Zinn, J.C.; Scolnic, D. Cosmic Distances Calibrated to 1% Precision with Gaia EDR3 Parallaxes and Hubble Space Telescope Photometry of 75 Milky Way Cepheids Confirm Tension with LambdaCDM. *arXiv* **2020**, arXiv:2012.08534.
25. Valentino, E.D.; Pan, S.; Yang, W.; Anchordoqui, L. A. Touch of neutrinos on the vacuum metamorphosis: Is the H_0 Solution Back? *Phys. Rev. D* **2021**, *103*, 123527. [CrossRef]
26. Banerjee, A.; Cai, H.; Heisenberg, L.; Colgain, E. O.; , Sheikh-Jabbari, M. M.; Yang, T. Hubble Sinks In The Low-Redshift Swampland. *Phys. Rev. D* **2021**, *103*, 081305. [CrossRef]
27. Capozziello, S.; Carloni, S.; Troisi, A. Quintessence without scalar fields. *Recent Res. Dev. Astron. Asrophys.* **2003**, *1*, 625.
28. Harko, T. Thermodynamic interpretation of the generalized gravity models with geometry-matter coupling. *Phys. Rev. D* **2014**, *90*, 044067. [CrossRef]
29. Bhardwaj, V.K.; Yadav, A.K. Some Bianchi type V accelerating cosmological models in $f(R,T) = f_1(R) + f_2(T)$ formalism. *Int. J. Geom. Meth. Mod. Phys.* **2020**, *7*, 2050159. [CrossRef]
30. Yadav, A.K.; Mondal, M.; Rahaman, F. Singularity-free nonexotic compact star in f(R,T) gravity. *Pramana J. Phys.* **2020,** *94*, 90. [CrossRef]
31. Sharma, L.K.; Yadav, ; A.K.; Singh, B.K. Power-law solution for homogeneous and isotropic universe in f(R, T) gravity. *New Astron.* **2020**, *79*, 101396. [CrossRef]
32. Singla, N.; Gupta, M.K.; Yadav, A.K. Accelerating model of flat universe in $f(R,T)$ gravity. *Grav. Cosmol.* **2020**, *26*, 144. [CrossRef]
33. Yadav, A. K.; Ali, A. T. Invariant Bianchi type I models in f(R,T) Gravity. *Int. J. Geom. Methods. Mod. Phys.* **2018**, *15*, 1850026. [CrossRef]
34. Yadav, A. K.; Srivastava, P. K.; Yadav, L. Hybrid expansion law for dark energy dominated universe in $f(R,T)$ Gravity. *Int. J. Theor. Phys.* **2015**, *54*, 1671. [CrossRef]
35. Hu, W.; Sawicki, I. Models of $f(R)$ cosmic acceleration that evade solar system tests. *Phys. Rev. D* **2007**, *76*, 064004. [CrossRef]

36. Nojiri, S.; Odintsov, S.D. Modified gravity with negative and positive powers of curvature: Unification of inflation and cosmic acceleration. *Phys. Rev. D* **2003**, *68*, 123512. [CrossRef]
37. Capozziello, S.; Cardone, V.F.; Troisi, A. Dark energy and dark matter as curvature effects. *JCAP* **2006** *0608*, 001.
38. Martins, C.F.; Salucci, P. Analysis of Rotation Curves in the framework of R^n gravity. *Mon. Not. R. Astron. Soc.* **2007**, *381*, 1103. [CrossRef]
39. Boehmer, C.G.; Harko, T.; Lobo, F. S. N. Dark matter as a geometric effect in $f(R)$ gravity. *Astropart. Phys.* **2008**, *29*, 386. [CrossRef]
40. Boehmer, C.G.; Harko, T.; Lobo, F.S.N. Generalized virial theorem in f(R) gravity. *JCAP* **2008**, *03*, 024. [CrossRef]
41. De Felice, A.; Tsujikawa, S. Construction of cosmologically viable $f(G)$ gravity models. *Phys. Lett. B* **2009**, *675*, 1. [CrossRef]
42. Bamba, K.; Odintsov, S.D.; Sebastiani, L.; Zerbini, S. Finite-time future singularities in modified Gauss-Bonnet and $F(R, G)$ gravity and singularity avoidance. *Eur. Phys. J. C* **2010**, *67*, 295. [CrossRef]
43. Bahamonde, S.; Zubair, M.; Abbas, G. Thermodynamics and cosmological reconstruction in $f(T, B$ gravity. *Phys. Dark Univ.* **2018**, *19*, 78. [CrossRef]
44. Nojiri, S.; Odintsov, S.D.; Oikonomou, V.K. Modified gravity theories on a nutshell: Inflation, bounce and late-time evolution. *Phys. Rept.* **2017**, *692*, 1. [CrossRef]
45. Oikonomou, V.K. Rescaled Einstein-Hilbert gravity from F(R) gravity: Inflation, dark energy, and the swampland criteria. *Phys. Rev. D* **2021**, *103*, 124028. [CrossRef]
46. Oikonomou, V.K. Unifying inflation with early and late dark energy epochs in axion F(R) gravity. *Phys. Rev. D* **2021**, *103*, 044036. [CrossRef]
47. Odintsov, S.D.; Oikonomou, V.K. Geometric inflation and dark energy with axion F(R) gravity. *Phys. Rev. D* **2020**, *101*, 044009. [CrossRef]
48. Odintsov, S.D.; Oikonomou, V.K. Unification of inflation with dark energy in F(R) gravity and axion dark matter. *Phys. Rev. D* **2019**, *99*, 104070. [CrossRef]
49. Yousaf, Z. Stellar filaments with Minkowskian core in the Einstein - Λ gravity. *Eur. Phys. J. Plus* **2017**, *132*, 71. [CrossRef]
50. Yousaf, Z. On the role of $f(G, T)$ terms in structure scalars. *Eur. Phys. J. Plus* **2019**, *134*, 245. [CrossRef]
51. Yousaf, Z.; Bamba, K.; Bhatti, M.Z. Causes of irregular energy density in f(R,T) gravity. *Phys. Rev. D* **2016**, *93*, 124048. [CrossRef]
52. Caldwell, R.R.; Dave, R.; Steinhardt, P.J. Cosmological Imprint of an Energy Component with General Equation of State. *Phys. Rev. Lett* **1998**, *80*, 1582. [CrossRef]
53. Ferreira, P.G.; Joyce, M. Cosmology with a primordial scaling field. *Phys. Rev. D* **1998**, *58*, 023503. [CrossRef]
54. Copel, E.J.; Liddle, A.R.; Wands, D. Exponential potentials and cosmological scaling solutions. *Phys. Rev. D* **1998**, *57*, 4686.
55. Liddle, A.R.; Scherrer, R.J. Classification of scalar field potentials with cosmological scaling solutions. *Phys. Rev. D* **1998**, *59*, 023509. [CrossRef]
56. Dodleson, S.; Kaplinghat, M.; Stewart, E. Solving the Coincidence Problem: Tracking Oscillating Energy. *Phys. Rev. Lett.* **2000**, *85*, 5276. [CrossRef]
57. Zlatev, I.; Wang, L.; Steinhardt, P.J. Quintessence, Cosmic Coincidence, and the Cosmological Constant. *Phys. Rev. Lett.* **1999**, *82*, 896. [CrossRef]
58. Steinhardt, P.J.; Wang L.; Zlatev, I. Cosmological tracking solutions. *Phys. Rev. D* **1999**, *59*, 123504. [CrossRef]
59. Johri, V.B. Search for tracker potentials in quintessence theory. *Class. Quant. Grav.* **2002**, *19*, 5959. [CrossRef]
60. Johri, V.B. Genesis of cosmological tracker fields. *Phys. Rev. D* **2001**, *63*, 103504. [CrossRef]
61. Sahni, V. Dark matter and dark energy. *Lect. Notes Phys.* **2004**, *653*, 141.
62. Sahni, V.; Starobinsky, A. The Case for a Positive Cosmological Lambda-term. *Int. J. Mod. Phys. D* **2000**, *9*, 373. [CrossRef]
63. Chimento, L.P.; Jakubi, A.S. Scalar field cosmologies with perfect fluid in Robertson-Walker metric. *Int. J. Mod. Phys. D* **1996**, *5*, 71. [CrossRef]
64. Hartle, J.B.; Hawking, S.W. Wave function of the Universe.*Phys. Rev. D* **1983**, *28*, 2960. [CrossRef]
65. Hawking, S.W. The quantum state of the universe. *Nucl. Phys. B* **1984**, *239*, 257. [CrossRef]
66. Vilenkin, A. Creation of universes from nothing. *Phys. Lett. B* **1982**, *117*, 25. [CrossRef]
67. Barvinsky, A.O. Unitarity approach to quantum cosmology. *Phys. Rep.* **1993**, *230*, 237. [CrossRef]
68. Spokoiny, B.L. Inflation and generation of perturbations in broken-symmetric theory of gravity. *Phys. Lett. B* **1984**, *147*, 39. [CrossRef]
69. Salopek, D.S.; Bond, J.R.; Bardeen, J.M. Designing density fluctuation spectra in inflation. *Phys. Rev. D* **1989**, *40*, 1753. [CrossRef]
70. Khalatnikov, I.M.; Mezhlumian, A. The classical and quantum cosmology with a complex scalar field. *Phys. Lett. A* **1992**, *169*, 308. [CrossRef]
71. Kamenshchik, A.Y.; Moschella, U.; Pasquier, V. An alternative to quintessence. *Phys. Lett. B* **2001**, *511*, 265. [CrossRef]
72. Gong, Y.; Zhang, Y. Probing the curvature and dark energy. *Phys. Rev. D* **2005**, *72*, 043518. [CrossRef]
73. Sharov, G.S.; Vasiliev, V.O. How predictions of cosmological models depend on Hubble parameter data sets. *Math. Model. Geom.* **2018**, *6*, 1. [CrossRef]
74. Biswas, P.; Roy, P.; Biswas, R. Posing constraints on the free parameters of a new model of dark energy EoS: Responses through cosmological behaviours. *arXiv* **2019**, arXiv:1908.00408.

75. Scolnic, D.M; Jones, D.O.; Rest, A.; Pan, Y.C.; Chornock, R.; Foley, R.J.; Huber, M.E.; Kessler, R.; Narayan, G.; Riess, A.G.; et al. The Complete Light-curve Sample of Spectroscopically Confirmed SNe Ia from Pan-STARRS1 and Cosmological Constraints from the Combined Pantheon Sample. *Astrophys. J.* **2018**, *859*, 101. [CrossRef]
76. Beutler, F.; Blake, C.; Colless, M.; Heath Jones, D.; Staveley-Smith, L.; Campbell L.; Parker, Q.; Saunders, W.; Watson F. The 6dF Galaxy Survey: Baryon acoustic oscillations and the local Hubble constant. *MNRAS* **2011**, *416*, 3017. [CrossRef]
77. Padmanabhan, N.; Xu, X.; Eisenstein, D. J.; Scalzo, R.; Cuesta, A. J.; Mehta, K. T.; Kazin, E. A 2 percent distance to $z = 0.35$ by reconstructing baryon acoustic oscillations - I. Methods and application to the Sloan Digital Sky Survey. *MNRAS* **2012**, *427*, 2132. [CrossRef]
78. Anderson, L.; Aubourg, E.; Bailey, S.; Bizyaev, D.; Blanton, M.; Bolton, A.S.; Brinkmann, J.; Brownstein, J.R.; Burden, A.; Cuesta, A.J.; et al. The clustering of galaxies in the SDSS-III Baryon Oscillation Spectroscopic Survey: Baryon acoustic oscillations in the Data Release 9 spectroscopic galaxy sample. *MNRAS* **2013**, *427*, 3435. [CrossRef]
79. Blake, C.; Brough, S.; Colless, M.; Contreras, C.; Couch, W.; Croom, S.; Davis, T.; Drinkwater, M. J.; Forster, K.; Gilbank, D.; Gladders, M.; et al. The WiggleZ Dark Energy Survey: The growth rate of cosmic structure since redshift $z = 0.9$. *MNRAS* **2011**, *415*, 2876. [CrossRef]
80. Hinshaw, G.; Larson, D.; Komatsu, E.; Spergel, D. N.; Bennett, C. L.; Dunkley, J.; Nolta, M. R.; Halpern, M.; Hill, R. S.; Odegard, N.; et al. Nine-year Wilkinson Microwave Anisotropy Probe (WMAP) Observations: Cosmological Parameter Results. *Astrophys. J. Suppl. Ser.* **2013**, *208*, 19. [CrossRef]
81. Bond, H.E.; Nelan, E.P.; VandenBerg, D.A.; Schaefer, G.H.; Harmer, D. HD 140283: A star in the solar neighborhood that formed shortly after big bang. *Astrophys. J.* **2013**, *765*, L12. [CrossRef]
82. Masi, S.; Ade, P.A.R.; Bock, J.J.; Bond, J.R.; Borrill, J.; Boscaleri, A.; Coble, K.; Contaldi, C.R.; Crill, B.P.; De Bernardis, P.; et al. The BOOMERanG experiment and the curvature of the universe. *Prog. Part. Nucl. Phys.* **2002**, 48, 243. [CrossRef]
83. Yadav, A.K.; Alshehri, A.M.; Ahmad, N.; Goswami, G.K.; Kumar, M. Transitioning universe with hybrid scalar field in Bianchi I space-time. *Phys. Dark Uni.* **2021**, *31*, 100738. [CrossRef]
84. Renzini, A.; Bragaglia, A.; Ferraro, F.R. The white dwarf distance to the globular cluster NGC 6752 (and its age) with the HUBBLE SPACE TELESCOPE. *Astrophys. J.* **1996**, *465*, L23. [CrossRef]
85. Valentino, E.D.; Anchordoqu, Luis A.; Akarsu, Ö.; Ali-Haimoud, Y.; Amendola, L.; Arendse, N.; Asgar, M.; Ballardini, M.; Basilakos, S.; Battistelli, E.; et al. Cosmology Intertwined IV: The Age of the Universe and its Curvature. *Astropart. Phys.* **2021**, 131, 102607. [CrossRef]
86. Capozziello, S.; Agostino, R. D.; Luongo, O. High-redshift cosmography: Auxiliary variables versus Pade polynomials. *Mon. Not. Roy. Astron. Soc.* **2020**, *494*, 2576. [CrossRef]
87. Cunha, C.E.; Lima, M.; Oyaizu, H.; Frieman, J.; Lin, H. Estimating the redshift distribution of photometric galaxy samples – II. Applications and tests of a new method. *Mon. Not. Roy. Astron. Soc.* **2009**, *396*, 2379. [CrossRef]
88. Jesus, J.F.; Valentim, R.; Escobal, A.A.; Pereira, S.H. Gaussian process estimation of transition redshift. *J. Cosm. Astrop. Phys.* **2020**, *04*, 053. [CrossRef]
89. Singla, N.; Gupta, M.K.; Yadav, A.K.; Goswami, G.K. Accelerating universe with binary mixture of bulk viscous fluid and dark energy. *Int. J. Mod. Phys. A* **2021**, *36*, 2150148. [CrossRef]
90. Prasad, R.; Gupta, L.K.; Yadav, A.K. Lyra's cosmology of homogeneous and isotropic universe in Brans-Dicke theory. *Int. J. Geom. Meth. Mod. Phys.* **2021**, *18*, 2150029. [CrossRef]
91. Prasad, R.; Gupta, L.K.; Beeshan, A.; Goswami, G.K.; Yadav, A.K. Bianchi type I universe: An extension of ΛCDM model. *Int. J. Geom. Meth. Mod. Phys.* **2021**, *18*, 2150069. [CrossRef]
92. Prasad, R.; Yadav, A.K.; Yadav, A.K. Constraining Bianchi type V universe with recent H(z) and BAO observations in Brans–Dicke theory of gravitation. *Eur. Phys. J. Plus* **2020**, *135*, 297. [CrossRef]
93. Sahni, V.; Saini, T.D.; Starobinsky, A.A.; Alam, U. Statefinder - a new geometrical diagnostic of dark energy. *JETP Lett.* **2003**, *77*, 201. [CrossRef]
94. Alam, U.; Sahni, V.; Saini, T.D.; Starobinsky, A.A. Exploring the Expanding Universe and Dark Energy using the Statefinder Diagnostic. *Mon. Not. R. Astron. Soc.* **2003**, *344*, 1057. [CrossRef]
95. Tsagas, C.G. The deceleration parameter in 'tilted' universes: Generalising the Friedmann background. *Euro. Phys. J. C* **2022**, *82*, 521. [CrossRef]
96. Bouali, A.; Chaudhary, H.; Debnath, U.; Roy, T.; Mustafa, G. Constraints on the Parameterized Deceleration Parameter in FRW Universe. *arXiv* **2023**, arXiv:2301.12107.
97. Macaulay, E.; Nichol, R. C.; Bacon, D.; Brout, D.; Davis, T. M.; Zhang, B.; Bassett, B. A.; Scolnic, D.; Moller, A.; D'Andrea, C. B. et al. First cosmological results using Type Ia supernovae from the Dark Energy Survey: Measurement of the Hubble constant. *arXiv* **2018**, arXiv:1811.02376.
98. Zhang, C.; Zhang, H.; Yuan, S.; Liu, S.; Zhang, T.J.; Sun, Y.C. Four New Observational H(z) Data From Luminous Red Galaxies of Sloan Digital Sky Survey Data Release Seven. *Res. Astron. Astrophys.* **2014**, *14*, 1221. [CrossRef]
99. Simon, J.; Verde, L.; Jimenez, R. Constraints on the redshift dependence of the dark energy potential. *Phys. Rev. D* **2005**, *71*, 123001. [CrossRef]
100. Stern, D.; Jimenez, R.; Verde, L.; Kamionkowski, M.; Stanford, S. A. Cosmic chronometers: Constraining the equation of state of dark energy I: H(z) measurements. *JCAP* **2010**, *1002*, 008. [CrossRef]

101. Moresco, M.; Cimatti, A.; Jimenez, R.; Pozzetti, L.; Zamorani, G.; Bolzonella, M.; Dunlop, J.; Lamareille, F.; Mignoli, M.; Pearce, H. et al. Improved constraints on the expansion rate of the Universe up to $z \sim 1.1$ from the spectroscopic evolution of cosmic chronometers. *JCAP* **2012**, *8*, 006. [CrossRef]
102. Gaztanaga, E.; Cabre, A.; Hui L. Clustering of Luminous Red Galaxies IV: Baryon Acoustic Peak in the Line-of-Sight Direction and a Direct Measurement of H(z). *MNRAS* **2009**, *399*, 1663. [CrossRef]
103. Chuang, D.H.; Wang, Y. Modelling the anisotropic two-point galaxy correlation function on small scales and single-probe measurements of H(z), $D_A(z)$ and $f(z)\sigma_8(z)$ from the Sloan Digital Sky Survey DR7 luminous red galaxies. *MNRAS* **2013**, *435*, 255. [CrossRef]
104. Alam, S.;Ata, M.; Bailey, S.; Beutler, F.; Bizyaev, D.; Blazek, J. A.; Bolton, A. S.; Brownstein, J. R.; Burden, A.; Chuang, C.-H. et al. The clustering of galaxies in the completed SDSS-III Baryon Oscillation Spectroscopic Survey: Cosmological analysis of the DR12 galaxy sample. *MNRAS* **2016**, *470*, 2617. [CrossRef]
105. Moresco, M.; Pozzetti, L.; Cimatti, A.; Jimenez, R.; Maraston, C.; Verde, L.; Thomas, D.; Citro, A.; Tojeiro, R.; Wilkinson, D.; A 6% measurement of the Hubble parameter at $z \sim 0.45$: Direct evidence of the epoch of cosmic re-acceleration. *JCAP* **2016**, *5*, 014. [CrossRef]
106. Blake, C.; Brough, S.; Colless, M.; Contreras, C.; Couch, W.; Croom, S.; Croton, D.; Davis, T.M.; Drinkwater, M.J.; Forster, K.; et al. The WiggleZ Dark Energy Survey: Joint measurements of the expansion and growth history at z < 1. *MNRAS* **2012**, *425*, 405.
107. Ratsimbazafy, A.L; Loubser, S.I.; Crawford, S.M.; Cress, C.M.; Bassett, B.A.; Nichol, R.C.; Vaisanen, P. Age-dating luminous red galaxies observed with the Southern African Large Telescope. *MNRAS* **2017**, *467*, 3239. [CrossRef]
108. Anderson, L.; Aubourg, É.; Bailey, S.; Beutler, F.; Bhardwaj, V.; Blanton, M. ; Bolton, Adam S.; Brinkmann, J.; Brownstein, Joel R.; Burden, A.; et al. The clustering of galaxies in the SDSS-III Baryon Oscillation Spectroscopic Survey: Baryon acoustic oscillations in the Data Releases 10 and 11 Galaxy samples. *MNRAS* **2014**, *441*, 24. [CrossRef]
109. Moresco, M. Raising the bar: New constraints on the Hubble parameter with cosmic chronometers at $z \sim 2$. *MNRAS* **2015**, *450*, L16. [CrossRef]
110. Busca, N. G; Delubac, T.; Rich, J.; Bailey, S.; Font-Ribera, A.; Kirkby, D.; Le Goff, J.-M.; Pieri, M. M.; Slosar, A.; Aubourg, É.; et al. Baryon acoustic oscillations in the Lyα forest of BOSS quasars. *Astron. Astrophys.* **2013**, *552*, A96. [CrossRef]
111. Rich, J.; Which fundamental constants for cosmic microwave background and baryon-acoustic oscillation?. *Astron. Astrophys.* **2015**, *584*, A69. [CrossRef]
112. Font-Ribera, A.; Kirkby, D.; Busca, N.; Miralda-Escude, J.; Ross, Nicholas P.; Slosar, A.; Rich1, J.; Aubourg, E.; Bailey, S.; Bhardwaj, V. et al. Quasar-Lyman α forest cross-correlation from BOSS DR11: Baryon Acoustic Oscillations *JCAP* **2014**, *1405*, 027. [CrossRef]